[19]The values of the constants are taken from the following sources: $\mu_N(Na^{23})$, H. F. Ramsey, Nuclear Moments, (John Wiley & Sons, Inc., New York, 1953); μ_B, a_B, and $\hbar$, R. B. Leighton, Principles of Modern Physics (McGraw-Hill Book Co., Inc., New York, 1959).
[20]Superscript ± will henceforth be used to denote one-electron spin states, both in the text and in the diagrams.
[21]Z. Kopal, Numerical Analysis (John Wiley & Sons, Inc., New York, 1961).
[22]T. Kjeldaas and W. Kohn, Phys. Rev. 101, 66 (1956).
[23]R. K. Nesbet, Quantum Theory of Atoms, Molecules and the Solid State, edited by P. O. Löwdin (Academic Press Inc., New York, 1966).
[24]G. D. Gaspari, W. M. Shyu, and T. P. Das, Phys. Rev. 134, A852 (1964).
[25]E. U. Condon, Rev. Mod. Phys. 40, 872 (1968).

PHYSICAL REVIEW A VOLUME 1, NUMBER 4 APRIL 1970

Electric Field Effect in the Resonance Lines of Indium and Thallium†

Thomas Richard Fowler* and Joseph Yellin
Lawrence Radiation Laboratory, University of California, Berkeley, California 94720
(Received 3 November 1969)

The atomic-beam method has been used to study the Stark effect in the resonance lines of indium ($6s\,^2S_{1/2} \rightarrow 5p\,^2P_{1/2}$, 4102 Å) and thallium ($7s\,^2S_{1/2} \rightarrow 6p\,^2P_{1/2}$, 3776 Å). The difference between the atomic polarizability of the $^2S_{1/2}$ state and that of the $^2P_{1/2}$ state [$\Delta\alpha(sp)$] has been determined and compared with calculations in the Coulomb approximation. For indium, we find $\Delta\alpha(sp) = 138(11) \times 10^{-24}$ cm^3 and for thallium $\Delta\alpha(sp) = 115(12) \times 10^{-24}$ cm^3.

I. INTRODUCTION

Although the perturbation of atomic levels by electric fields was first observed more than forty years ago,[1] there has been little progress by way of a systematic study of the Stark effect on free atoms until the present decade. This has been due to the experimental difficulties of measuring small frequency shifts and attaining high electric fields, as well as theoretical difficulties in calculating and interpreting experimental results. Unlike the Zeeman effect, which depends only on the angular part of the wave function and can be calculated accurately for any atomic state, the calculation of the Stark effect involves infinite sums of radial integrals requiring accurate radial wave functions for excited states.

Recently, there has been a resurgence of interest in the electric field effect. The renewed activity is due to the successful application of new experimental techniques to the Stark effect and to theoretical developments. In addition, interest has been generated by the application of the Stark effect to the search for electric dipole moments in elementary particles,[2–4] and the measurement of isotope shifts[5] and hyperfine structure of excited states.[6,7] On the experimental side, atomic-beam[8] level-crossing,[9,10] and optical double-resonance[11] techniques have been used to observe differential Stark shifts between levels of an atomic state as well as shifts between levels belonging to two different states (optical Stark shift).[12] To observe the differential shifts within a state $\approx 10^{-8}$ to 10^{-6} Hz/(kV cm^{-1})^2, relatively low electric fields (< 100 kV/cm) are required on account of the precision attainable in radiofrequency spectroscopy. To observe and measure the Stark shift in optical transitions requires large electric fields (> 100 kV/cm), which are required because of the linewidths associated with optical transitions and the calibration procedure, which involves large Stark shifts of approximately 10^3 MHz. Thus techniques had to be developed for achieving high electric fields. On the theoretical side, methods have been developed for treating the infinite sums appearing in the Stark effect[13,14] and calculating the radial integrals needed.[15]

In the present experiment, the atomic-beam method was used to investigate the Stark shift in the 4102 Å line of indium and the 3776 Å line of thallium. This experiment serves as an important preliminary to the measurement of isotope shifts in indium by the atomic-beam method.

II. EXPERIMENTAL METHOD

The experimental method employed here has been described previously in connection with the Stark-shift measurements in the D_1 lines of cesium, rubidium, and potassium.[12,16] The application of the

method to indium and thallium deserves some additional discussion owing to the different energy-level structure; hence, we will review the methods using indium as an example. The basic idea is one of a tuning experiment in which optical absorption lines of beam atoms are tuned by an electric field to emission lines of the same atoms. The atomic-beam apparatus is used to detect the spin-flip which accompanies tuning. For a description of the atomic-beam apparatus, we refer to the literature.[17]

An atomic-beam apparatus with flop-in geometry is employed. In the C region, a pair of electric field plates replaces the usual C magnet, and an optical photon source (resonance lamp) replaces the usual radiofrequency photon source (signal generator). The electric field plates may be used to select a particular m_J trajectory, and we assume this to be the case. Such state selection simplifies the analysis, but is not necessary and was not used in this experiment.

Imagine a beam of indium atoms in the ground-state level $|5^2P_1/2 m_J = -\frac{1}{2}\rangle$ in the C region and with no electric field present. The energy-level diagram is shown in Fig. 1. If the atoms are illuminated with resonance radiation 4102 Å, they will be excited to the $6s\ ^2S_{1/2}$ state and decay back ($\tau = 7.5\times10^{-9}$ sec) to the $^2P_{1/2}$ state as well as to the metastable $^2P_{3/2}$ state. It is clear that of those atoms returning to the $^2P_{1/2}$ state, one-half will be in the $m_J = +\frac{1}{2}$ level and will thus be refocused at the detector. Some of the atoms terminating in the $^2P_{3/2}$ state will also undergo transitions $m_J = -\frac{1}{2}$ to $m_J = +\frac{1}{2}$, however, due to the different gJ of the $^2P_{3/2}$ state, these atoms will not be deflected properly and we may ignore them for the present. Thus, with no electric field applied in the C region, a flop-in signal is observed at the detector. To consider what happens when an electric field is applied to the beam atoms we have to take the hyperfine structure into account. The hyperfine structure associated with the 4102 Å line of indium[18, 19] is shown in Fig. 1. Also, reference to the Breit-Rabi diagram shows us that 90% of the indium atoms are in the lower ($F=4$) hyperfine state prior to being flopped. We neglect the remaining 10% for simplicity and assume that all the atoms are in the $F=4$ hyperfine state. The beam atoms then have two hyperfine absorption lines while the lamp emission line has four hyperfine components. The situation is depicted in Fig. 2(a). Application of an electric field to the beam atoms decreases the transition frequencies of the lines α' and β', detuning them from α and β. α' and β' are decreased by the same amount within the approximation described in the next section. Hence, the flop-in signal diminishes. However, for the appropriate values of the electric field, α' and β' can be brought into resonance with other hyperfine components, as shown in Fig. 2. Each time that α' or β' is made coincident with an emission line component the flop-in signal increases. The frequency shifts associated with each of the diagrams in Fig. 2 and the electric fields at which they occur are shown in Table I. Similar results hold for thallium ($I=\frac{1}{2}$) except that the β component of the hyperfine transitions is forbidden, and hence fewer resonances occur. The energy-level diagram for thallium is shown in Fig. 1. The possible resonances for thallium are shown in Fig. 3 and summed up in Table II.

III. THEORY

In this section, we obtain an expression for the Stark shift $\Delta\nu_S$ in an optical line. A comprehensive treatment of the Stark effect may be found in the literature.[1, 20]

The interaction of an atom with an external electric field E directed along the z axis is described by the Hamiltonian

$$\mathcal{H}_1 = e\sum_i [rC_0^1(\theta,\phi)]_i E \ , \qquad (1)$$

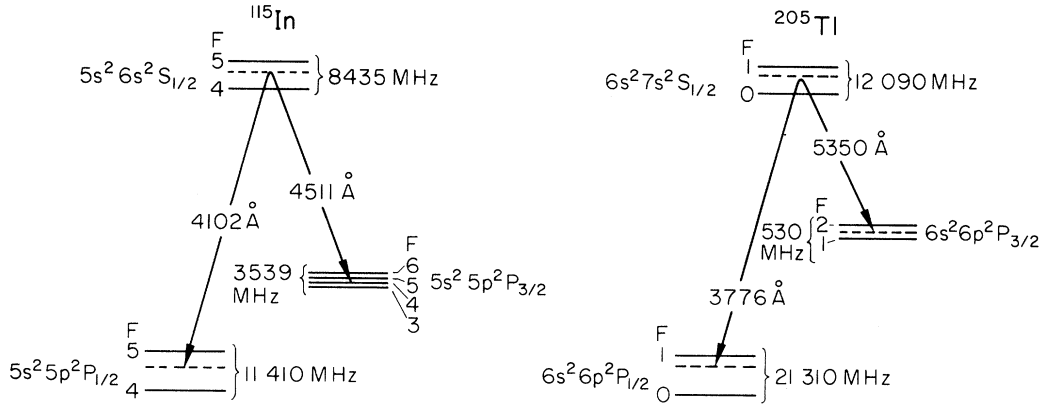

FIG. 1. Indium and thallium energy levels.

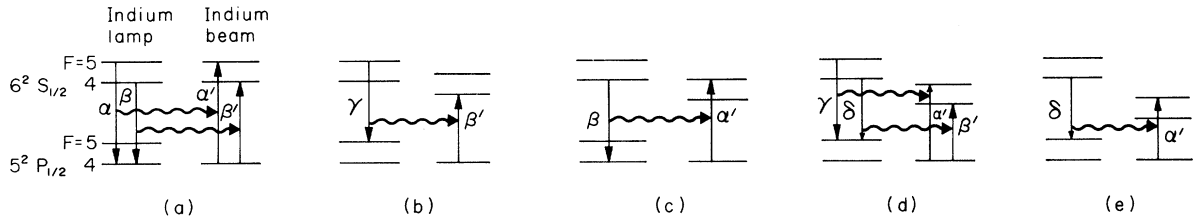

FIG. 2. Possible overlaps between absorption lines of indium beam atoms (primed) and indium lamp lines (unprimed).

TABLE I. Frequency shifts, electric fields, and signal intensities associated with indium.

Indium			$F=4$			$F=5$	
Overlapping lines	$\alpha'=\alpha$ $\beta'=\beta$	$\beta'=\gamma$	$\alpha'=\beta$	$\alpha'=\gamma$ $\beta'=\delta$	$\alpha'=\delta$	$\gamma'=\gamma$ $\delta'=\delta$	$\gamma'=\delta$
$\Delta\nu_S$(MHz)	0	2974	8435	11410	19845	0	8435
Approx. kV/cm	0	162	274	319	425	0	274
Signal intensity	1.132	0.242	0.364	1.030	1.000	1.444	0.667

where we have expressed the position vector of the ith electron, $\vec{r}_i$, in terms of the spherical tensors $C_q^1(\theta,\phi)$.[21] We treat $\mathcal{H}_1$ as a perturbation on the atomic Hamiltonian which includes the central field, spin-orbit, and hyperfine structure operators.

The hyperfine interaction is included since

$$\Delta\nu_S(^2P_{1/2}) \ll \Delta\nu_{hf}(^2P_{1/2}) ,$$

and $$\Delta\nu_S(^2S_{1/2}) \approx \Delta\nu_{hf}(^2S_{1/2})$$

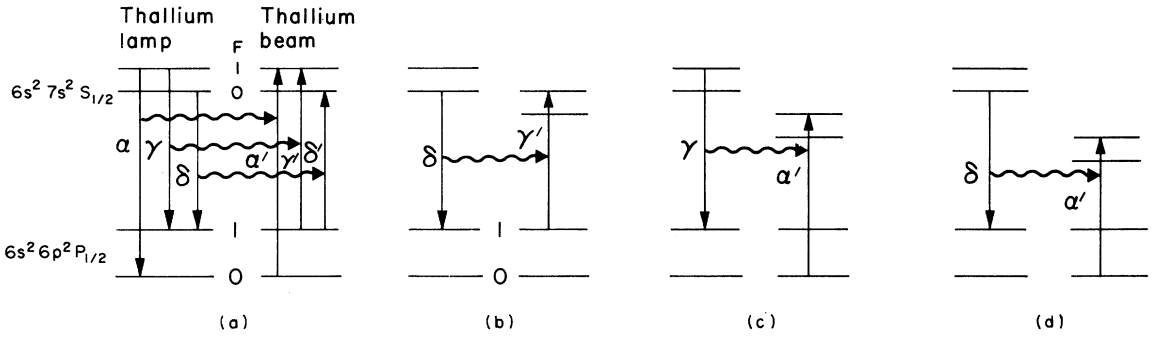

FIG. 3. Possible overlaps between absorption lines of thallium beam atoms (primed) and thallium lamp lines (unprimed).

TABLE II. Frequency shifts, electric fields, and signal intensities associated with thallium.

Thallium	No state selection			
Overlapping lines	$\alpha'=\alpha$ $\gamma'=\lambda$, $\delta'=\delta$	$\gamma'=\delta$	$\alpha'=\gamma$	$\alpha'=\delta$
$\Delta\nu_S$(MHz)	0	12090	21311	33401
Approx. kV/cm	0	366	485	610
Signal intensity	1.50	0.50	0.50	0.25

for both indium and thallium.

The first nonvanishing contribution of $\mathcal{H}_1$ to the energy is given by second-order perturbation theory:

$$\Delta\nu_S(\gamma F m_F)=\frac{e^2E^2}{h}\sum_{\gamma' F'} \times\sum_i \frac{|\langle\gamma' F' m_F|(rC_0^1)_i|\gamma F m_F\rangle|^2}{\Delta W(\gamma' F',\gamma F)} , \quad (2)$$

where $\Delta W(\gamma' F',\gamma F)=W(\gamma' F')-W(\gamma F)$.

Considerable simplification can be achieved by considering the magnitude of the hyperfine structure and hyperfine Stark effect[20] in relation to the energies of the electronic configurations and the Stark shifts induced in the electronic configurations. We note first that $\Delta W(\gamma' F',\gamma F)$ differs from the energy denominator without hyperfine structure $\Delta W(\gamma',\gamma)$ by order $(\Delta\nu_{\rm hf})/(\Delta\nu_{\rm opt})\approx 10^{-5}$, and hence the hyperfine structure may be neglected in ΔW. Next we examine the hyperfine structure Stark effect. The frequency shifts induced by an electric field in the hyperfine transition $(F=0, m_F=0)\rightarrow(F=1, m_F=0)$ of the $6p\,^2P_{1/2}$ state of ^{205}Tl have been measured and are given by $\delta(\Delta\nu)\cong 3\times10^{-7}E^2$ Hz, where E is in V/cm.[22] Similar results may be expected in other transitions in the $^2P_{1/2}$ state as well as the $^2S_{1/2}$ state. This is to be compared with the frequency shift induced by an electric field in the electronic transition $6s^2(^1S)7s\rightarrow 6s^2(^1S)6p$ of thallium which can be readily estimated to be $\delta[\Delta\nu(6p-7s)]\sim 10^{-1}E^2$ Hz, and to the linewidths $\approx 10^9$ Hz inherent in the present experiment. Similar remarks apply to indium. Thus, for the purposes of this experiment, hyperfine structure effects may be neglected. All hyperfine states are displaced by the same amount by the application of an electric field. The amount by which they are displaced depends only on the electronic quantum numbers within the above approximations, and is given by

$$\Delta\nu_S(\alpha J m_J)=\frac{e^2E^2}{h}\sum_{\alpha' J'} \times\sum_i \frac{|\langle\alpha' J' m_J|(rC_0^1)_i|\alpha J m_J\rangle|^2}{\Delta W(\alpha' J',\alpha J)} . \quad (3)$$

In the present case, we are dealing with a single electron coupled to a $^1S_0$ core; therefore, to the extent that the transition electron does not polarize the core,

$$\Delta\nu_S(nljm_j)=\frac{e^2E^2}{h}\sum_{n'l'j'}(2l+1)(2l'+1)(2j+1)(2j'+1)\begin{Bmatrix} l' & l & 1\\ j & j' & s\end{Bmatrix}^2\begin{pmatrix} j' & j & 1\\ m_j & -m_j & 0\end{pmatrix}^2 \times\begin{pmatrix} l' & l & 1\\ 0 & 0 & 0\end{pmatrix}^2\frac{|\langle n'l'j'\|r\|nlj\rangle|^2}{\Delta W(n'l'j',nlj)} . \quad (4)$$

A number of authors have evaluated the angular factors in Eq. (3) for particular values of ljm_j,[23,24] but in fact we can reduce Eq. (3) to a simple formula that sums up the Stark effect for any alkalilike transitions. For, due to the selection rules on l and j and remembering that j equals $l\pm\frac{1}{2}$, there are at most three nonvanishing terms in the angular part of the summation. Furthermore, the $3j$ and $6j$ coefficients are of a particularly simple kind and may be readily expressed in terms of their arguments. Thus, we arrive at

$$\Delta\nu_S(nlj=l\pm\tfrac{1}{2}m_j)=\frac{e^2E^2}{4h}\left(\frac{j^2-m_j^2}{j^2}R(l-1,j-1;nlj)+\frac{m_j^2}{j^2(j+1)^2}R(l\pm1,j;nlj)+\frac{(j+1)^2-m_j^2}{(j+1)^2}R(l+1,j+1;nlj)\right) , \quad (5)$$

where $R(l-1,j-1;nlj)$

$$=\sum_{\substack{n'\\ n'\neq n}}\frac{|\langle n'l-1,j-1\|r\|nlj\rangle|^2}{\Delta E(n'l-1,j-1;nlj)} ,$$

and similarly for the other terms. The $\pm$ in the second term on the right-hand side is to be used with $j=l\pm\frac{1}{2}$.

Applying Eq. (5) to an $s_{1/2}$ and a $p_{1/2}$ state,[25] we get:

$$\Delta\nu_S(ns_{1/2})=\frac{e^2E^2}{9h}[R(p_{1/2};ns_{1/2})+2R(p_{1/2};ns_{1/2})] ,$$

$$\Delta\nu_S(np_{1/2})=\frac{e^2E^2}{9h}[R(s_{1/2};np_{1/2})+2R(d_{3/2};np_{1/2})] ,$$

or for the shift in the optical line $n_1s_{1/2} \leftrightarrow n_2p_{1/2}$

$$\delta(n_1s_{1/2} \leftrightarrow n_2p_{1/2}) = \frac{e^2E^2}{9h}\{R(s_{1/2}; n_2p_{1/2}) - R(p_{1/2}; n_1s_{1/2}) + 2[R(d_{3/2}; n_2p_{1/2}) - R(p_{3/2}; n_1s_{1/2})]\} \ .$$

If we define the atomic polarizability as usual by $h\Delta\nu_S = -\frac{1}{2}\alpha E^2$, then

$$2\delta(n_1s_{1/2} \leftrightarrow n_2p_{1/2})hE^{-2} = \Delta\alpha(n_2p_{1/2}; n_1s_{1/2}) \ ,$$

where

$$\Delta\alpha(n_2p_{1/2}; n_1s_{1/2}) = \alpha(n_2p_{1/2}) - \alpha(n_1s_{1/2}) \ .$$

IV. APPARATUS

The atomic-beam apparatus is conventional, except for the electric field plates, and will not be discussed here. The electric field plates, the high-voltage power supply, and the associated read-out equipment have been described previously, and no further discussion is needed.[26] We limit our discussion to the beam source, detector, and light sources.

A. Production and Detection of Beams

Beams of indium and thallium were produced by electron bombardment of a tantalum oven containing indium or thallium and having a 0.030-in. slit. Approximately 30 W (electron bombardment) were required to produce thallium beams and 60 W were required for indium. The oven temperature was not measured, but was estimated at approximately 1200 °K. The populations of the metastable $^2P_{3/2}$ state can be calculated from the Boltzmann factors and are negligible for thallium, while about 15% of the indium atoms are in the $^2P_{3/2}$ state.

Detection of indium and thallium was accomplished with an iridium hot-ribbon surface ionization detector $1\times0.1\times0.0015$ in. Iridium was used because of its high work function (5.9 eV) and the fact that it is inherently quieter and less troublesome than the more usual surfaces. Typical background from the hot ribbon was around 2×10^{-12} A with a noise $< 10^{-13}$ A. A Keithy 417 high-speed picoammeter was used to measure the ion currents.

B. Resonance Lamps

The measurement of the Stark effect by atomic beams requires light sources having a high spectral density. Since the atomic beam is illuminated at right angles to its direction, the absorption width of beam atoms is the natural width $\Delta\nu_N \sim 10$ MHz. The light source must put out enough photons within this width to flop a substantial number of atoms. An intense electrodeless discharge lamp was developed for this purpose.

The low vapor pressure of indium makes it impractical to discharge the metal directly; consequently, indium iodide was used. The high vapor pressure of iodine, which is produced in the dissociation of the iodide, causes the discharge to become unstable, so it is necessary to use microscopic amounts of the iodide in order to limit the iodine vapor pressure. To this end the iodide was formed in the presence of an argon discharge so that formation of the iodide could be monitored through the appearance of the indium blue line. The procedure is similar to that used by Cunningham and Link[27] with two exceptions: (i) We distilled the indium to insure purity; and (ii) We reacted the indium with iodine prior to sealing off the lamp. After forming the iodide, the argon was pumped out and the lamp refilled with spectroscopic grade xenon at a pressure of 1 Torr and sealed off. The thallium lamp presented no special problem and thallium chloride was used.

The quartz lamps were cylinders 5 cm diam and 6 mm long. They were outgassed under vacuum at around 900 °C for at least 10 h before filling. The pressure prior to filling was approximately 2×10^{-7} Torr.

Excitation of the lamps was achieved with a 100-W diathermy unit with a type-A antenna. The lamp to be excited was placed in an oven, one end of which consisted of the microwave antenna. A boron nitride holder fixed the lamp inside the oven. A schematic of the oven is shown in Fig. 4. Normally the diathermy unit was operated at 60 to 80% power and the lamp temperature maintained about 210 °C for indium and about 240 °C for thallium. The lamp profiles were scanned with the atomic-beam apparatus as previously described. A scan of the indium lamp line is shown in Fig. 5, where the frequency scale has been established from the known hyperfine structure of the $5p\ ^2P_{1/2}$ and $6s\ ^2S_{1/2}$ states.[18, 19, 28] The intensity distribution shown is actually a composite since a number of absorption lines are simultaneously scanning the lamp. It is clear from the width of the lamp line that less than $\frac{1}{2}$% of the available light is effective in pumping the beam.

V. EXPERIMENTAL RESULTS

The measurement of the Stark shift consists in scanning the lamp line with the atomic-beam apparatus, as previously described, identifying the various resonances and using them to determine the frequency shift as a function of the applied

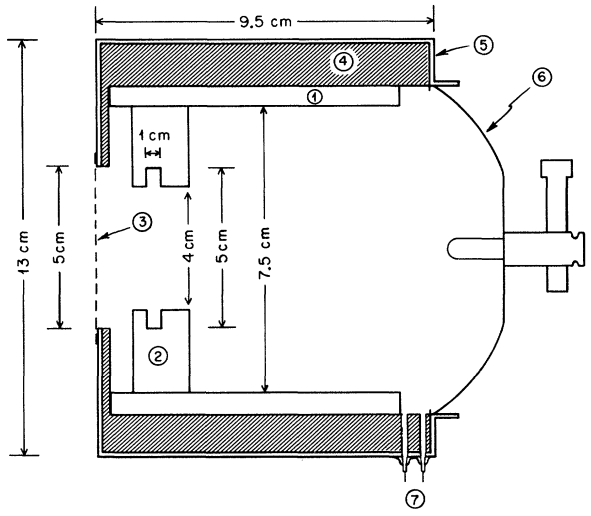

FIG. 4. Details of the indium and thallium lamp oven: (1) Heavy Duty, Inc. heater, (2) boron nitride lamp holder, (3) copper screen, (4) asbestos, (5) copper shell, (6) type-A antenna, (7) electrical feedthrough.

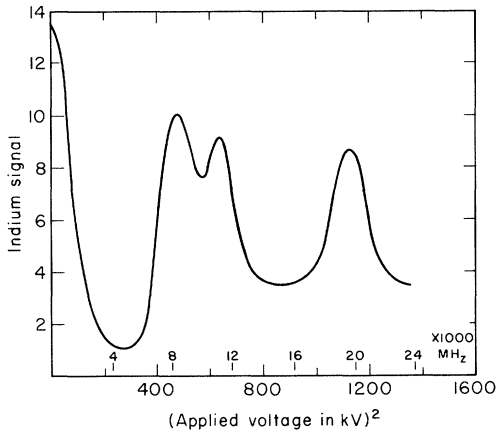

FIG. 5. Indium Stark-shift data. Overlapping lines are indicated above the resonances. The frequency scale is established from the known hyperfine structure of the 4102 Å line of indium.

voltages V. All that remains to be done is measure the electric field gap, d, and determine the electric field from V/d. The illumination region is sufficiently small compared to the dimensions of the plates that fringing effects may be neglected. Details of the plates were previously published.[26] The voltages were supplied by a Sams[29] 50-kV supply and read by a digital voltmeter using a Parks[30] voltage divider. Over-all accuracy of the voltage system was $< 0.1\%$. The electric-field gap was measured with a feeler gauge which was checked against a micrometer. The value of the gap was $d = 0.825 \pm 0.024$ mm. We present below, separately, the results for indium and thallium.

A. Indium

Typical results for indium are shown in Fig. 5 and are summarized in Table III in terms of the polarizability difference $\Delta\alpha(6^2S_{1/2}, 5^2P_{1/2})$. Also shown are the theoretical values of the polarizabilities which are based on Eq. (5) and the Bates-Damgaard (BD) Coulomb approximation, which was used to calculate the radial integrals.

The resonance lamp and beams were made from naturally occurring indium. In natural abundance, indium consists of two isotopes ^{115}In (96%) and ^{113}In (4%). The hyperfine structure of these isotopes differs by ≈ 25 MHz [28] and may be neglected for our purposes. The isotope shift ≈ 270 MHz [31] is a small fraction of the linewidth and may be neglected particularly in view of the low abundance of ^{113}In.

Two features of Fig. 5 are rather conspicuous and deserve comment; first, the absence of a peak at 2974 MHz, and second, the near equality of the three high-field peaks. These features can be understood with reference to the last row of Table I, where we show the signal intensities. The signal intensities are calculated by multiplying together the transition probabilities of overlapping lines. Theoretical transition probabilities were used. We see that if we did not select the $F = 4$ hyperfine state but instead had both the $F = 4$ and $F = 5$ hyperfine states present in the beam (no state selection) the signal intensity at 2974 MHz would be $\approx 9\%$ of the zero electric-field signal intensity. In view of the linewidth, we would not expect to observe this peak. Furthermore, the signal intensities at 8435, 11 410, and 19 845 MHz would be equal. Indeed, due

TABLE III. Summary of calculated and experimental polarizabilities.

	Theoretical polarizabilities[a] $\times 10^{24}$ cm^{-3}					Experimental
	$\alpha(^2P_{1/2})$	$\alpha(^2P_{3/2}\pm\frac{3}{2})$	$\alpha(^2P_{3/2}\pm\frac{1}{2})$	$\alpha(^2S_{1/2})$	$\Delta\alpha(^2S_{1/2}, ^2P_{1/2})$	$\Delta\alpha(^2S_{1/2}, ^2P_{1/2})$
Indium	4.7	4.5	7.4	150.8	146.1	138(11)
Thallium	2.7	4.4	9.0	125.0	122.3	115(12)

[a] Bates-Damgaard.

to the small $g_J = 0.67$ of the $^2P_{1/2}$ state and the high velocity of the beam atoms, state selection cannot be accomplished with the size of the electric-field gap employed.

B. Thallium

Results for thallium are shown in Fig. 6 and summarized in Table III. All measurements were made using naturally occurring thallium, which consists of two isotopes ^{203}Tl (30%) and ^{205}Tl (70%). Here the isotope shift is a large fraction of the linewidth amounting to ≈ 1600–1800 MHz, [32, 33] and consequently the thallium resonances are broader. The difference in the hyperfine structure[34] (≈ 200 MHz) which could lead to a more complicated pattern may be neglected.

The experimental results are in good agreement with BD calculations but were found to be lower than BD by ≈ 6% in all measurements.[35] We can obtain a reasonably good value for $\alpha(^2P_{1/2})$ by relating α to the oscillator strengths f, and using experimental f values. If we use the f values of Penkin and Shabanova,[36] we get for indium and thallium, respectively, $\alpha(5^2P_{1/2}) = 4.5(1.5)\times10^{-24}$ cm^3 and $\alpha(6^2P_{1/2}) = 3.5(1)\times10^{-24}$ cm^3. From these values of the ground-state polarizabilities, we can deduce the excited-state polarizabilities. We get, for indium and thallium, respectively, $\alpha(6^2S_{1/2}) = 142(12.5)\times10^{-24}$ cm^3 and $\alpha(7^2S_{1/2}) = 118(13)\times10^{-24}$ cm^3 in very good agreement with DB (Table III). We have calculated also the polarizabilities of the metastable state, $\alpha(^2P_{3/2} \pm m_j)$, from the f values of Penkin and Shabanova and find them to be in fair agreement with the BD values.

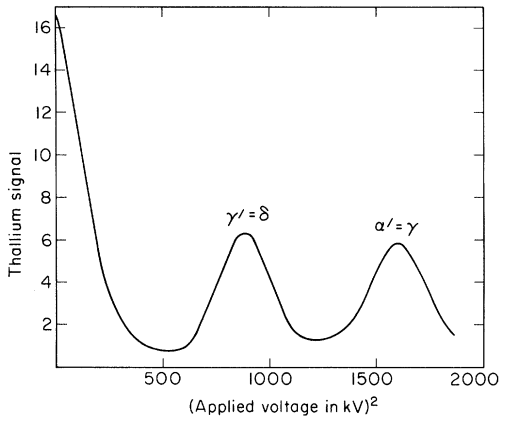

FIG. 6. Thallium Stark-shift data. Overlapping lines are indicated above the resonances.

ACKNOWLEDGMENTS

The authors gratefully acknowledge the interest of Professor Richard Marrus. We are grateful to Professor Howard Shugart and to Dr. Edmond Geneux for reading the manuscript and discussing the results.

†Work performed under the auspices of the U. S. Atomic Energy Commission.

*Present address: Logicon Inc., San Pedro, Calif.

[1]For a review of recent literature on the Stark effect see A. M. Bonch-Bruevich and V. A. Khodovoi, Usp. Fiz. Nauk. 93, 71 (1967) [English transl.: Soviet Phys. – Usp. 10, 637 (1968)].

[2]P. G. H. Sandars and E. Lipworth, Phys. Rev. Letters 13, 718 (1964).

[3]G. E. Harrison, P. G. H. Sanders, and S. J. Wright, Phys. Rev. Letters 22, 1263 (1969).

[4]V. W. Cohen, R. Nathans, H. B. Silsbee, E. Lipworth, and N. F. Ramsey, Phys. Rev. 177, 1942 (1969).

[5]R. Marrus and D. McColm, Phys. Rev. Letters 15, 813 (1965).

[6]R. Marrus, E. Wang, and J. Yellin, Phys. Rev. Letters 19, 1 (1967).

[7]T. H. Duong, R. Marrus, and J. Yellin, Phys. Letters 27B, 565 (1968).

[8]R. D. Haun and J. R. Zacharias, Phys. Rev. 107, 107 (1957).

[9]B. Budick, S. Marcus, and R. Novick, Phys. Rev. 140, A1041 (1965).

[10]A. Khadjavi, W. Happer, Jr., and A. Lurio, Phys. Rev. Letters 17, 463 (1966).

[11]J. Blamont, Ann. Phys. (Paris) 2, 551 (1957).

[12]R. Marrus, D. McColm, and J. Yellin, Phys. Rev. 147, 556 (1966).

[13]R. M. Sternheimer, Phys. Rev. 96, 951 (1954).

[14]C. Schwartz, Ann. Phys. (N.Y.) 6, 156 (1956).

[15]D. R. Bates and A. Damgaard, Phil. Trans. Roy. Soc. (London) A242, 101 (1949).

[16]R. Marrus and J. Yellin, Phys. Rev. 177, 127 (1969).

[17]N. F. Ramsey, Molecular Beams (Oxford University Press, London, 1956).

[18]G. V. Deverall, K. W. Meissner, and G. J. Zissis, Phys. Rev. 91, 297 (1953).

[19]D. A. Jackson, Proc. Roy. Soc. (London) 241A, 283 (1957).

[20]J. R. P. Angel and P. G. H. Sandars, Proc. Roy. Soc. (London) A305, 125 (1968).

[21]A. R. Edmond, Angular Momentum in Quantum Mechanics (Princeton University Press, Princeton, N.J., 1957).

[22]G. Palmer, J. R. Peterson, and R. C. Mockler, Bull. Am. Phys. Soc. 12, 905 (1967).

[23]K. Murakawa and M. Yamamoto, J. Phys. Soc. Japan 20, 1057 (1965);

[24]I. Miyachi and K. J. Ram, J. Phys. B2, 425 (1969).
[25]In Ref. 23, the authors take the radial integrals of the fine-structure states to be the same and hence the resulting formulas differ. This assumption may not be justified when the spin-orbit interaction is large.
[26]R. Marrus, E. Wang, and J. Yellin, Phys. Rev. 177, 122 (1969).
[27]P. T. Cunningham and J. K. Link, J. Opt. Soc. Am. 57, 1000 (1967).
[28]T. G. Eck, A. Lurio, and P. Kusch, Phys. Rev. 106, 954 (1957).
[29]Giannini-Voltex, Whittier, Calif.
[30]Singer Metrics Division, The Singer Company, Bridgeford, Conn.
[31]D. A. Jackson, Phys. Rev. 101, 1425 (1956); 105, 1925 (1957).
[32]D. A. Jackson, Z. Phys. 75, 223 (1932).
[33]C. J. Schuler, M. Ciftan, L. C. Bradley, III, and H. H. Stroke, J. Opt. Soc. Am. 52, 501 (1962).
[34]A. Lurio and A. G. Prodell, Phys. Rev. 101, 79 (1956).
[35]Calculations were performed directly from the *B-D* theory using a computer program written by Dr. Allen Lurio, math and computing department of the Lawrence Radiation Laboratory.
[36]N. P. Penkin and L. N. Shabanova, Optics and Spectr. 14, 5 (1963); 14, 87 (1963).

PHYSICAL REVIEW A VOLUME 1, NUMBER 4 APRIL 1970

Integral-Transformation Trial Functions of the Fractional-Integral Class

R. L. Somorjai
Division of Chemistry, National Research Council of Canada, Ottawa 7, Canada
and
David M. Bishop
Department of Chemistry, University of Ottawa, Ottawa 2, Canada
(Received 24 November 1969)

We propose fractional integrals (Euler transforms) of conventional quantum-mechanical functions as special integral-transform trial functions. Calculations on the first four members of the He isoelectronic sequence with three different-order Euler transforms of both Slater and Gaussian 1*s* orbitals are reported. A pilot calculation for H_2 with an Euler transform of an LCGTO (linear combination of Gaussian-type orbitals) molecular orbital gives a total energy $E=-1.10903$ a.u. at $R=1.4$ a.u. (exact value is -1.17444 a.u.). A generalization of the shape function used in this work is given and the general applicability of Euler transforms discussed.

INTRODUCTION

A new class of trial functions has recently been introduced by one of us.[1] These functions are generated by the integration over the appropriately weighted "scale factor space" of conventional trial functions. We refer to the weight functions $S(t)$ for these integral-transform trial functions as shape functions[2]; the mathematical problem is the determination of $S(t)$.

Instead of attempting to solve the generally difficult integral equation that a given $S(t)$ satisfies, we took the simpler approach of parametrizing some *preselected* $S(t)$ and optimizing its parameters variationally. Simple arguments suggest[2] that a trial $S(t)$ should be a δ-convergent sequence[3]; there is still however the problem of choosing an appropriate yet tractable sequence.

In this paper, we propose a class of sequences, simple in form, which generate trial functions that can be expressed by well-known fractional integrals.[4]

FRACTIONAL INTEGRAL TRANSFORMS

The Riemann-Liouville fractional integral of $f(x)$ is defined by[4]

$$g(y;\mu)\equiv\mathfrak{R}_\mu[f(x);y]$$

$$=\Gamma^{-1}(\mu)\int_0^y f(x)(y-x)^{\mu-1}dx\ , \qquad (1)$$

and the corresponding Weyl fractional integral by